Journal of Thermal Analysis and Calorimetry (2020) 141:751–766
https://doi.org/10.1007/s10973-019-09049-z

A thermal analysis and physicochemical study on thermoresponsive chimeric liposomal nanosystems

Nikolaos Naziris[1] · Athanasios Skandalis[2] · Aleksander Forys[3] · Barbara Trzebicka[3] · Stergios Pispas[2] · Costas Demetzos[1]

Received: 6 June 2019 / Accepted: 10 November 2019 / Published online: 25 November 2019

Abstract

Thermoresponsive nanomaterials have led to a plethora of new applications in the fields of Nanobiotechnology, Biomedicine and Therapeutics. Since liposomal membranes are lyotropic liquid crystals, the development of thermoresponsive liposomes for drug delivery has been recognized as an attractive scientific field. Additionally, plenty of studies utilizing the temperature-dependent response of certain synthetic polymers are conducted, alone or in combination with liposomes. In the present study, we combined the liposomal and thermoresponsive polymer technologies, in order to create functional chimeric/mixed liposomal nanosystems with innovative properties. Initially, differential scanning calorimetry was applied on chimeric/mixed bilayers to evaluate the effect of polymeric guests on the thermotropic behavior of lipidic membranes. Thereafter, chimeric/mixed liposomes were built and their physicochemical properties, as well as their colloidal stability were measured and evaluated. The nature of the self-assembled structures and the lipidic membrane morphology were investigated through cryo-transmission electron microscopy, while their thermoresponsiveness and its consequences on the lipidic membrane properties were assessed, through a simple heating protocol. The presence of a new thermodynamic phase on the lipidic membrane acts as an agglomeration and aggregation inducer, affecting the whole colloidal chimeric/mixed nanosystem. This mechanism might be characterized as "phase functionality" and may be utilized for drug delivery purposes and also in other applications. Biophysics and thermodynamics are very important tools to study the self-assembly process, as well as the stability and bio-functionality of drug delivery systems.

Keywords Chimeric liposomes · Thermoresponsiveness · Thermal analysis · Light scattering · Cryo-TEM · Phase functionality

Introduction

Functional advanced drug delivery nanosystems (aDDnSs) have gained considerable attention, because they can be used as stimuli-responsive nanoplatforms, incorporating bioactive molecules. In the recent years, the responsive behavior of nanosystems has been achieved by applying the "chimeric" concept for developing innovative drug nanocarriers. In this context, the incorporation of stimuli-responsive polymers inside conventional systems and lipidic nanoplatforms, such as liposomes, is used to build chimeric/mixed nanoparticles [1, 2]. Thermoresponsive/thermosensitive liposomes have been introduced in clinical phase III for the delivery of doxorubicin to primary liver cancer, under the trademark Thermodox® [3, 4]. However, stimuli-responsive liposomes are lately developed by attaching functional polymers onto the liposomal membrane and this approach is promising

Electronic supplementary material The online version of this article (https://doi.org/10.1007/s10973-019-09049-z) contains supplementary material, which is available to authorized users.

✉ Costas Demetzos
demetzos@pharm.uoa.gr

[1] Section of Pharmaceutical Technology, Department of Pharmacy, School of Health Sciences, National and Kapodistrian University of Athens, Panepistimioupolis Zografou, 15771 Athens, Greece

[2] Theoretical and Physical Chemistry Institute, National Hellenic Research Foundation, 48 Vassileos Constantinou Avenue, 11635 Athens, Greece

[3] Centre of Polymer and Carbon Materials, Polish Academy of Sciences, 34 M. Curie-Skłodowskiej St., 41-819 Zabrze, Poland

for effective control of the membrane disruption and consequently, release of the drug molecule or the therapeutic moiety in a spatiotemporal way. As a result, the bioavailability of drugs is increased and accumulation in healthy tissues is minimized, resulting in enhanced effectiveness and safety of these nanomedicines [5, 6].

Thermoresponsive polymers belong to the class of "smart biomaterials," and their intensive study is expected to deliver novel and revolutionary therapeutic approaches. Their unique behavior is "encoded" during their synthesis and hidden inside certain functional chemical groups. These groups are sensitive to heating or cooling at certain temperature ranges, interacting with each other or with the environment, which leads to alteration of the molecular physicochemical characteristics on various levels, such as their hydrophilic-to-hydrophobic balance and spatial conformation. Thermoresponsiveness is exploited to build "smart nanodevices" for the diagnosis, monitoring and treatment of various diseases, including the release of drug molecules in specific disease sites, such as tumors, and in specific kinetic manners. This is achieved either by developing nanoparticles composed of thermoresponsive polymers, e.g., micelles or polymersomes, or by integrating them on other nanotechnological platforms, in a way that combines their structural benefits and responsive properties benefits. An example application of the latter is polymer-modified thermosensitive liposomes (TSLs) [7, 8].

PNIPAM is a thermoresponsive polymeric molecule that comprises hydrophilic and hydrophobic domains and is considered as the most investigated "smart thermoresponsive material." Its solubility in water depends on temperature, due to the characteristic lower critical solution temperature (LCST), initially described as a parameter that induces phase separation when heating the aqueous solution above 32 °C [9]. The thermoresponsive behavior of PNIPAM is attributed to the temperature-dependent alteration in hydrogen bonding between the side chain amide groups and the surrounding solute molecules in the microenvironment. Below LCST, the functional groups are in a hydrated state, whereas above LCST, there is low affinity of these groups for water molecules, making the polymer less hydrophilic [10, 11]. The driving force for this "hydrophobic effect" is the entropy of water, and the LCST is an entropically driven property [12]. The result of hydrophobicity is that the polymer transits from an extended coil state to a shrunk globular state when heated above the LCST [13]. This utility enables for building a wide range of technological platforms for biomedical purposes, such as thermoresponsive controlled delivery of bioactive molecules, gene delivery, tissue engineering, self-healing, bioimaging and other applications. In particular, the thermo-reversible phase transition of PNIPAM and its derivatives have been extensively utilized for hydrogel development and find application even in three-dimensional bioprinting [14]. Other types of PNIPAM-based systems include micelles, polymersomes, films and particles [15]. What is more, the LCST of PNIPAM and related biomaterials can be tailored and adjusted close to physiological temperature values (37 °C), by copolymerization with other hydrophilic or hydrophobic monomers, control of the molecular weight and architecture and finally, control of the overall hydrophilicity of the final molecule [16, 17].

Thermal analysis is the first step to rationally design chimeric/mixed liposomal nanosystems, by predicting the stability of nanoparticles that will occur from the self-assembly of phospholipids and polymers, also assessing the functionality that the stimulus-responsive polymer will impart to the liposomal membrane [18, 19]. Various membrane phenomena are the result of the thermotropic effect that "foreign" biomaterials bring about on the dynamic phospholipid assembly, altering its phase behavior and fluidity, inducing phase separation and creating new metastable phases [20]. In any case, the lyotropism of these nanomaterials is the main protagonist, since their relative concentration inside the aqueous medium has shown to be of primary importance [21, 22]. The effect of guest biomaterials on the thermotropic behavior of bilayers and liposomes has been extensively investigated by DSC, with respect to the nature and concentration of these molecules. Examples include drug molecules, proteins, dendrimers, amphiphilic polymers and carbon nanomaterials, aiming either to build liposomal drug nanocarriers or to exploit phospholipid bilayers as model membranes and evaluate the biophysical effect of certain molecules on them [23–26]. On top of these, thermoresponsive polymers are expected to promote the creation of innovative thermotropic properties inside chimeric membranes that could lead to thermoresponsiveness and consequently, bio-functionality of the developed nanosystems [27]. In this scenario, thermodynamics is expected to delineate the interactions between these biomaterials, providing a prediction of the final structure stability and functionality, while together with biophysics, they constitute the building blocks of aDDnSs [28].

The scope of this work was to integrate the technology of thermoresponsive amphiphilic polymers into the liposomal platform, through the development of chimeric/mixed nanosystems and evaluation of their functional properties on a thermodynamic basis. The results of this work might be used as technological background for evaluating thermoresponsive chimeric/mixed liposomal nanosystems as drug delivery carriers. The chimeric/mixed nanosystems comprised phospholipids, specifically 1,2-dipalmitoyl-sn-glycero-3-phosphocholine (DPPC) or of L-α-phosphatidylcholine (Egg, Chicken) (EPC) and thermoresponsive amphiphilic diblock copolymers, namely poly(*N*-isopropylacrylamide)-b-poly(lauryl acrylate) (PNIPAM-b-PLA) 1 or 2 (Fig. 1). DPPC is characterized by a gel-to-liquid crystalline phase

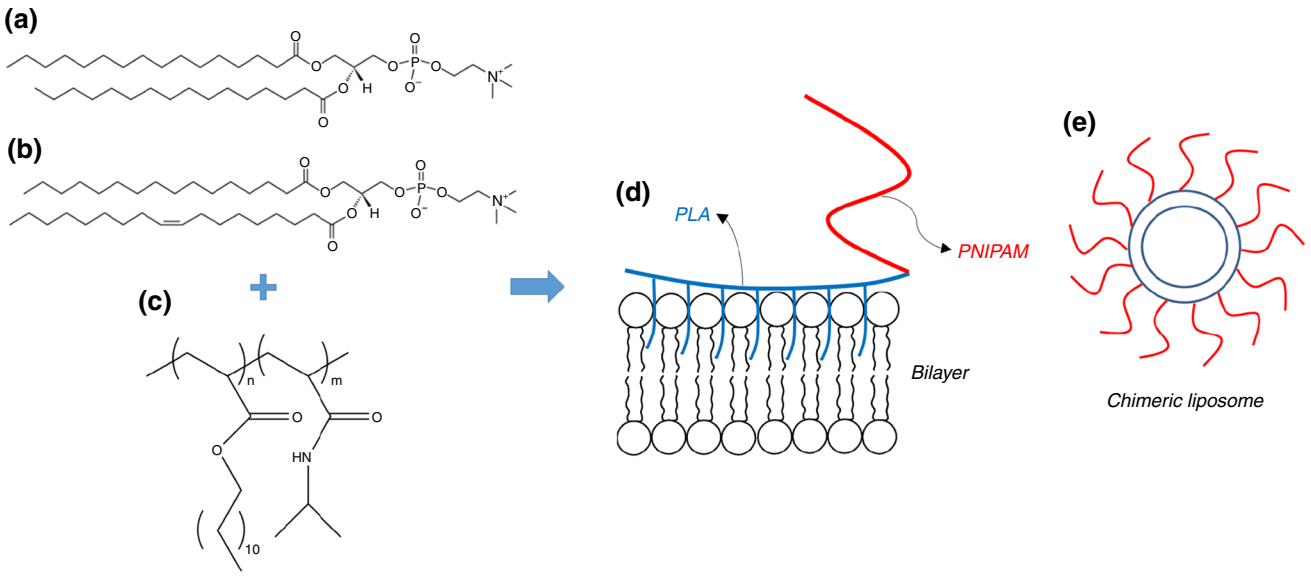

Fig. 1 Molecular structures of **a** DPPC, **b** EPC and **c** PNIPAM-b-PLA 1 (with *n*:*m* weight ratio being 34:64) or 2 (with *n*:*m* weight ratio being 50:50) and the resulting chimeric/mixed **d** bilayers and **e** liposomes comprised of phospholipid and thermoresponsive amphiphilic diblock copolymer

transition (T_m) of around 41 °C, while EPC melts at very low temperatures, evidently at − 5 °C [29, 30]. Considering the copolymers, they were composed of a different number and ratio of PNIPAM and PLA segments and as a result, they differed in composition and molecular weight (M_w). PNIPAM-b-PLA 1 was 66–34% w/w in composition, with $M_w = 18{,}000$, while PNIPAM-b-PLA 2 was 50–50% w/w, with $M_w = 6400$, making it richer in hydrophobic PLA and shorter in length as a macromolecule. The difference in nature of these molecules allowed for evaluation of their lyotropic effect on the liposomal membrane, based on their hydrophilic-to-hydrophobic balance and size. The herein utilized techniques provided a picture of the interactions that take place in both the hydrophobic and the polar regions of the membranes, with the PLA segment being the polymer anchor that stabilizes the membrane, while PNIPAM extends outside the membrane and provides colloidal stability and functionality. In addition, the copolymers contained a carboxyl end group –COOH at the PLA block free end. The effect of these polymer molecules on liposomal membranes was evaluated through various techniques.

Materials and methods

Materials

The saturated phospholipid 1,2-dipalmitoyl-sn-glycero-3-phosphocholine (DPPC) and phospholipid mixture of L-α-phosphatidylcholine (Egg, Chicken) (EPC) were purchased from Avanti Polar Lipids Inc. (Alabaster, AL, USA) and used without further purification (Fig. 1a, b). They each have molecular weight of 734.039 and 770.123, respectively, according to product description. DPPC has two 16:0 lipid chains 16:0 and its main transition temperature (T_m) is around 41 °C, while EPC is a phospholipid mixture that reportedly melts at − 5 °C. Chloroform and other reagents were of analytical grade and purchased from Sigma-Aldrich Chemical Co. The poly(*N*-isopropylacrylamide)-b-poly(lauryl acrylate) (PNIPAM-b-PLA) thermoresponsive amphiphilic diblock copolymers were synthesized in two different weight compositions, 66–34% w/w for PNIPAM-b-PLA 1 and 50–50% w/w for PNIPAM-b-PLA 2 (Fig. 1c). The M_w of copolymers equals to 18,000 and 6400, respectively.

Synthesis of PNIPAM-based Thermoresponsive Amphiphilic Diblock Copolymers

The reversible addition–fragmentation chain-transfer (RAFT) polymerization methodology was used to synthesize the PNIPAM-b-PLA 1 and 2 copolymers, which were further characterized by size exclusion chromatography (SEC) and nuclear magnetic resonance spectroscopy (NMR). More details on the block copolymer synthesis by RAFT are provided in our previous works [19]. The weight-average molecular weights M_w of PLA and PNIPAM blocks were 5800 and 12,200 (18,000 total) for PNIPAM-b-PLA 1 and 3900 and 2500 (6400 total) for PNIPAM-b-PLA 2,

respectively. Polydispersity index (M_w/M_n) of the copolymers was 1.55 and 1.16, respectively.

Preparation of Lipidic and Chimeric/Mixed Bilayers

Pure lipid and chimeric bilayers were prepared for DSC analysis by mixing the appropriate amounts of DPPC and PNIPAM-b-PLA 1 or 2 (9:0.02, 9:0.05, 9:0.1, 9:0.2, 9:0.5 and 9:1 molar ratios) in chloroform solutions and subsequently evaporating the solvent under vacuum and heat conditions, through a rotary evaporator (Rotavapor R-114, Buchi, Switzerland). Chimeric phospholipid/block copolymer films were formed by removing the solvent at 40 °C. The films were maintained under vacuum for 30 min, and then in a desiccator, for at least 24 h, in order to remove traces of solvent.

Differential Scanning Calorimetry (DSC)

DSC experiments were carried out by utilizing an 822^{e}Mettler-Toledo (Schwerzenbach, Switzerland) calorimeter, calibrated with pure indium ($T_m = 156.6$ °C). Sealed aluminum crucibles of 40 μL capacity were used as sample holders. Fully hydrated bilayers were investigated. This was achieved by placing 3.0 mg of each sample in a crucible, hydrating with 20 μL of phosphate-buffered saline (PBS), sealing and leaving samples to anneal for 30 min. Two heating–cooling cycles and a third heating scan were performed, in order to ensure good reproducibility of the data, with an empty aluminum crucible as reference. The temperature range was between 20 and 60 °C, while the scanning rate was 5 °C min^{-1}, under constant nitrogen gas flow rate of 50 mL min^{-1}. Before each cycle, the samples were subjected to a constant temperature of 20 °C for 10 min, in order to ensure equilibration. The calorimetric data obtained (characteristic transition temperatures $T_{onset,m/s/t}$ and $T_{m/s/t}$, enthalpy changes $\Delta H_{m/s/t}$ and widths at half peak height of the C_p profiles $\Delta T_{1/2,m/s/t}$) were analyzed with Mettler-Toledo STAR ^{e} software. All transition enthalpies were normalized per total biomaterial mass, including phospholipid and polymer. Furthermore, the correlation between polymer concentration and the transition specific enthalpy values for each polymer was investigated through scatter analysis, using "Microsoft Office EXCELL." For this purpose, the R-squared values were assessed.

Preparation of Lipidic and Chimeric/Mixed Vesicles

Liposomal systems of DPPC or EPC and PNIPAM-b-PLA 1 or 2 were prepared, by utilizing the thin-film hydration method. Specifically, appropriate amounts of lipid and lipid/polymer (9:0.02, 9:0.05, 9:0.1 and 9:0.5 molar ratios) were dissolved in chloroform and then transferred into a round flask, connected to a rotary evaporator (Rotavapor R-114, Buchi, Switzerland). Vacuum was applied, and thin films were formed by slow removal of the solvent at 40 °C. Thereafter, they were maintained under vacuum for at least 24 h in a desiccator, in order to remove possible traces of solvent. Afterward, they were hydrated with PBS (pH = 7.4), by slow stirring for 1 h in a water bath, above the phase transition temperature of the containing phospholipid (45 °C for DPPC and 25 °C for EPC). The final total biomaterial concentration of the liposomal systems was 5 mg mL^{-1} in every case. The resultant suspensions were subjected to two 5 min sonication cycles (amplitude 70%, cycle 0.5 s), interrupted by a 5-min resting period, by using a probe sonicator (UP 200S, dr. Hielsher GmbH, Berlin, Germany). The resultant chimeric systems were allowed to anneal for 30 min.

Light Scattering Techniques

The size, size distribution and zeta potential of the obtained liposomes were investigated by dynamic and electrophoretic light scattering (DLS and ELS, respectively). The physicochemical characteristics were measured immediately after preparation ($t = 0$ days), as well as over a 10-day period for DPPC liposomes and 30-day period for EPC liposomes, to monitor the colloidal system physical stability. For DLS and ELS, aliquots were diluted 30-fold in HPLC-grade water. Measurements were performed at a detection angle of 90° and at 25 °C, in a photon correlation spectrometer (Zetasizer 3000 HSA, Malvern, UK) and analyzed by the CONTIN method (MALVERN software).

Cryogenic Transmission Electron Microscopy (cryo-TEM)

Cryo-TEM micrographs were obtained using a Tecnai F20 TWIN X microscope (FEI Company, USA), equipped with field emission gun, operating at an acceleration voltage of 200 kV. Images were recorded on the Eagle 4 k HS camera (FEI Company, USA) and processed with TIA software (FEI Company, USA). Specimen preparation was done by vitrification of the aqueous (HPLC-grade water) suspensions on grids with holey carbon film (Quantifoil R 2/2; Quantifoil Micro Tools GmbH, Germany). Prior to use, the grids were activated for 15 s in oxygen plasma using a Femto plasma cleaner (Diener Electronic, Germany). Cryo-samples were prepared by applying a droplet (3 μL) of the suspension to the grid, blotting with filter paper and immediate freezing in liquid ethane using a fully automated blotting device Vitrobot Mark IV (FEI Company, USA). After preparation, the vitrified specimens were kept under liquid nitrogen until they were inserted into a cryo-TEM-holder Gatan 626 (Gatan Inc., USA) and analyzed in the TEM at − 178 °C.

Heating of Thermoresponsive Liposomes

In order to study the thermoresponsive behavior of the developed chimeric nanosystems, samples were placed in the oven, at 45 °C for 30 min, then left to reach room temperature and measured for their size and polydispersity with DLS, after 30-fold dilution in HPLC-grade water. Next, they were subjected to two 5-min probe sonication cycles, interrupted by a 5-min resting period; they were left to anneal and measured again for size and polydispersity. Finally, they were again placed in the 45 °C environment, so as to evaluate the reproducibility of the process.

Statistical Analysis

DLS and ELS results are shown as mean value ± standard deviation (S.D.) of three independent measurements. Statistical analysis was performed using Student's *t* test, and multiple comparisons were done using one-way ANOVA. *P* values < 0.05 were considered statistically significant. All statistical analyses were performed using "Microsoft Office EXCELL."

Results and discussion

DSC Analysis on Chimeric Bilayers

Differential scanning calorimetry (DSC) was conducted on polymer-grafted chimeric/mixed bilayers, composed of the phospholipid DPPC, which is an extensively studied phospholipid in terms of thermal analysis, and each one of the thermoresponsive amphiphilic diblock copolymers PNIPAM-b-PLA 1 and 2. The DSC heating curves for the DPPC:PNIPAM-b-PLA systems are presented in Figs. 2 and 3, while the respective thermodynamic parameter values are listed in Tables 1–4. Scatter analysis for both polymers is presented in Fig. 4. The plots between transition enthalpy and polymer molar ratio for the 1st and 2nd heating scans are available in the supporting information section, in Figure S1, while the corresponding cooling curves and cooling thermodynamic parameter values are provided in Figure S2 to S3 and Table S1 to S2.

Initially, the heating and cooling curves of DPPC membranes were obtained in PBS, as references for the chimeric systems. At first glance, the three heating curves of DPPC were almost identical to each other, with totally reproducible phase transitions. Those were the pretransition from gel ($L_{\beta'}$) to rippled ($P_{\beta'}$) phase and the main transition from rippled ($P_{\beta'}$) to liquid crystalline phase (L_{α}). The thermodynamic parameters of these phase transitions are in line with the literature, if we take into consideration the effect of hydration medium, which in our case is PBS, on phospholipid mesophase behavior [31]. Specifically, the main transition enthalpy is approximately 45 J g^{-1}, which translates to 33 kJ mol^{-1} or 7.9 kcal mol^{-1} of DPPC. As expected, the cooling process exhibited slightly higher transition enthalpy, a slight hysteresis, as well as lack of pretransition [32].

Considering the incorporation of PNIPAM-b-PLA 1, with molecular weight 18,000 and relative block composition 66–34%, inside DPPC bilayers, the thermodynamic effect of increasing amounts of the copolymer is presented in Fig. 2 and Tables 1 and 2. What we observe at first is that for chimeric systems there is a great difference between the curves of the 1st and 2nd heating scans (Fig. 2a, b) and, respectively, a deviation in the thermodynamic parameter

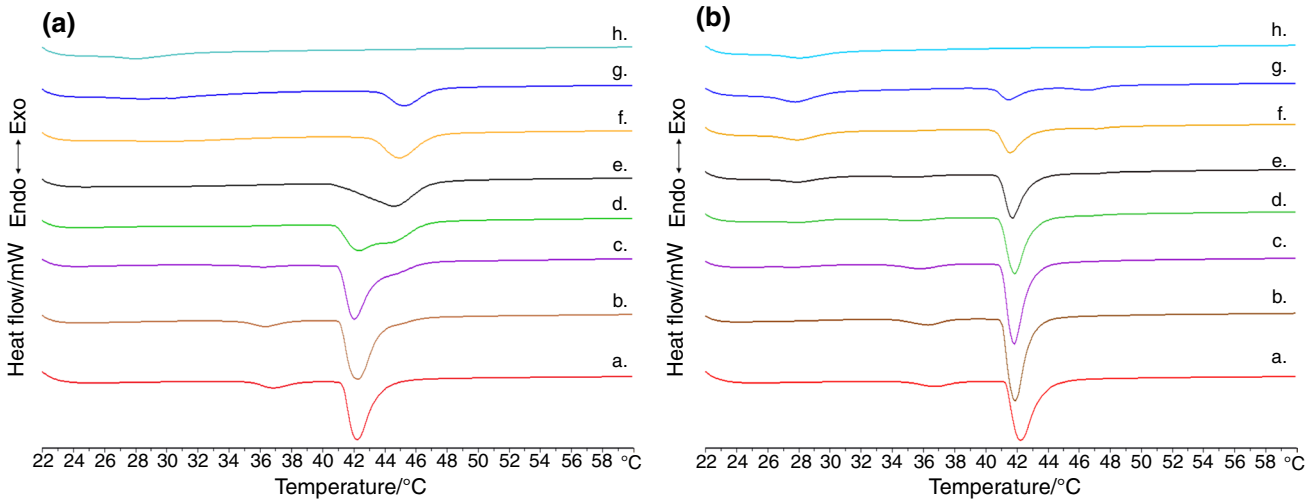

Fig. 2 DPPC:PNIPAM-b-PLA 1 **a** 1st and **b** 2nd DSC heating cycles for systems (a) DPPC and DPPC:PNIPAM-b-PLA 1 (b) 9:0.02, (c) 9:0.05, (d) 9:0.1, (e) 9:0.2, (f) 9:0.5, (g) 9:1 and (h) PNIPAM-b-PLA 1

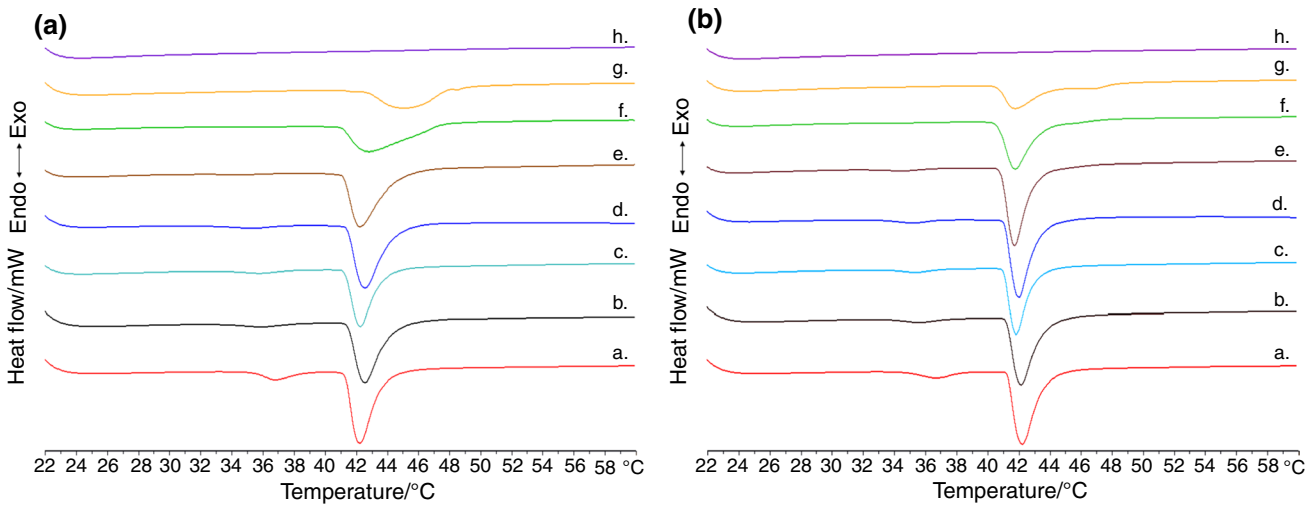

Fig. 3 DPPC:PNIPAM-b-PLA 2 **a** 1st and **b** 2nd DSC heating cycles for systems (a) DPPC and DPPC:PNIPAM-b-PLA 2 (b) 9:0.02, (c) 9:0.05, (d) 9:0.1, (e) 9:0.2, (f) 9:0.5, (g) 9:1 and (h) PNIPAM-b-PLA 2

values of the main transition. After that, the 3rd heating scan (data not shown) was exactly the same with the 2nd, which confirms that the systems reached equilibrium after the 1st heating and phase transition. This difference between the 1st and the 2nd proceeding heating processes was polymer concentration dependent, becoming much clearer in the cases of high polymer concentration inside the bilayer, especially above 9:0.1. Apparently, by gradually adding amounts of polymer, the main transition of DPPC is decreased, with reduced peak height and enthalpic content, giving its place to a new phase, which is of different organization and stability, leading to higher transition temperature [20, 24]. This phase begins as a shoulder to the DPPC main transition at low polymer concentrations and prevails at higher ones, i.e., 9:0.2 and above. However, after the 1st heating, the thermoresponsive copolymer rearranges inside the membrane and disrupts it, leading to a phase that is very similar to the reference one, only lower on transition specific enthalpy, depending again on polymer concentration. The displacement of the main transition from higher temperature to lower and the decrease in enthalpic content are due to the polymer molecules that rearranged inside the lipid membranes during the first transition, disturbed the membranes and disrupted the bilayers [6, 33]. The concentration-dependent enthalpy decrease between scans is expected, since the higher the membrane polymer content, the more the groups of PLA inside and groups of PNIPAM around the membrane that respond to heat and promote perturbation and disruption. As a result, the polymer amount is the cause for both the creation of a new, non-equilibrium/metastable and non-reversible phase and at the same time, the reason for thermoresponsive membrane disruption and reduced energetic content. We could say that the newly formed phase is a functional and thermoresponsive phase, which alters greatly the thermodynamic profile of the membrane after the 1st heating process. The plots between transition specific enthalpy (ΔH_m) and the concentration of the incorporated polymer for both scans are provided in Figure S1A. The deviation between 1st and 2nd heating cycles is apparent from molar ratio 9:0.5 and above. In addition, correlation analysis between polymer molar ratio inside the nanosystem and transition specific enthalpy revealed that the enthalpy decreases in a logarithmic manner as polymer amount is increased from 0.05 to 1 (Fig. 4a).

In addition, the pretransition of DPPC disappeared for molar ratios above 9:0.05, indicating interaction of the copolymer with the polar head groups of phospholipids and reduction of their mobility [18]. However, this occurred only for the 1st heating scan and the pretransition peak reappeared during the 2nd and 3rd scans for certain systems that contained low polymer amount, meaning that the polar head group mobility was restored after one heating cycle. The interesting phenomenon here is that although we did not observe a pretransition for 9:1, a low enthalpy peak appeared above the main transition during the 2nd and 3rd scans, which is probably associated with the non-equilibrium thermoresponsive phase that was recorded for the 1st heating. Finally, another type of phase transition was the one close to the LCST of PNIPAM, which was recorded at around 28 °C. Particularly, this transition occurred during the 1st scan for chimeric nanosystems with molar ratio 9:0.5 and 9:1 (1.63 J and 4.65 J per g of total sample or 77 kJ and 173 kJ per mol of PNIPAM), as well as for the tested neat polymer sample (5.84 J g^{-1} or 159 kJ mol^{-1}), but during the next scans, not only it appeared for 9:0.1 and 9:0.2, but it also increased in enthalpic content for the aforementioned systems. Specifically, if calculated per total sample

Table 1 Calorimetric profiles of DPPC:PNIPAM-b-PLA 1 chimeric bilayers in PBS (pH = 7.4) (1st heating cycle)

Sample	Molar ratio	$T_{onset,m}$/°C	T_m/°C	$\Delta T_{1/2,m}$/°C	ΔH_m/J g^{-1}	$T_{onset,s}$/°C	T_s/°C	$\Delta T_{1/2,s}$/°C	ΔH_s/J g^{-1}	$T_{onset,t}$/°C	T_t/°C	$\Delta T_{1/2,t}$/°C	ΔH_t/J g^{-1}
Lipid	–	41.04	41.80	1.44	−44.60	35.16	36.62	1.86	−5.81	–	–	–	–
Chimeric	9:0.02	40.88	41.90	1.68	−52.88	34.54	36.12	1.80	−5.32	–	–	–	–
Chimeric	9:0.05	40.83	41.64	1.56	−51.05	34.06	35.95	1.99	−1.84	–	–	–	–
Chimeric	9:0.1	40.65	42.07	3.94	−44.72	–	–	–	–	–	–	–	–
Chimeric	9:0.2	40.66	44.42	3.43	−39.28	–	–	–	–	–	–	–	–
Chimeric	9:0.5	42.92	44.76	2.30	−25.55	–	–	–	–	27.13	30.07	3.94	−1.63
Chimeric	9:1	43.43	44.99	2.07	−17.00	–	–	–	–	25.72	28.71	4.31	−4.65
Polymer	–	–	–	–	–	–	–	–	–	25.65	27.97	3.08	−5.84

T_{onset}: temperature at which the thermal event starts; T: temperature at which heat capacity (ΔC_p) at constant pressure is maximum; $\Delta T_{1/2}$: width at half peak height of the transition; ΔH: transition enthalpy normalized per gram of chimeric system. m: main transition; s: secondary transition; t: thermoresponsive transition

weight, chimeric system 9:1 exceeded the polymer sample (10.42 J g^{-1} vs. 7.03 J g^{-1}) and if calculated per moles of PNIPAM, all systems from 9:0.1 to 9:1 showed increased enthalpy values (232 to 388 kJ mol^{-1} vs. 192 kJ mol^{-1}). This is a new phase that is created after the 1st heating, which is strongly associated with the LCST of PNIPAM. It has been proposed in our previous investigation that this may be due to lateral diffusion of the incorporated polymer and phase separation into polymer-rich and polymer-poor domains [20, 34]. In this case, the membrane phase is determinant for the polymer conformation inside the bilayer, where the transition from gel-to-liquid crystalline phase may allow for polymer redistribution and domain formation [35]. It is indeed highly unlikely that this transition is owed purely to the polymer, because of the fact that its concentration is very low (0.33 mM for 9:0.1 to 3.3 mM for 9:1), compared with neat polymer solution (5.8 mM) or compared with other DSC studies on this molecule and only interactions between polymer and membrane could create such a phase [36]. The additive effect of PBS-contained salts on the LCST of PNIPAM was also manifested on the thermotropic behavior of the chimeric systems. In specific, it has been documented that the Hofmeister anions, such as chloride and phosphate ones, affect the phase transition of the polymer in a linear way, depending on their concentration, as well as on the polymer M_w. In this case, the concentration of chloride anions (0.14 M) brings about the greater effect; however, the rest of the salts contribute as well, resulting in the observed PNIPAM-related phase transition of the membranes being around 28 °C [37].

As a result, it is evident that the incorporated amount of polymer creates a new functional phase inside the phospholipid membrane, which is thermoresponsive and when heated, it disrupts the lipid bilayer and allows the copolymer to diffuse, leading to phase segregation and creating new domains or self-assembly into polymeric aggregates through its hydrophobic PLA segment [6, 33, 38]. This transition and consequent effects are polymer concentration dependent, since the systems with higher amount of polymer reduced more the main transition enthalpy after the 1st heating cycle and also exhibited a thermoresponsive phase transition of higher enthalpy than the others. At higher polymer concentrations, we observe that the energy of the main transition is reduced between the two first cycles and simultaneously, the pretransition of DPPC appears and the thermoresponsive transition associated with the LCST of PNIPAM is increased. We could say that energy is transferred from one phase to the others. The lyotropic and thermotropic effect of the utilized biomaterial on phase creation and "phase functionality" is most evident in the case of DPPC:PNIPAM-b-PLA 1 9:1, where thermoresponsiveness through phase transition led to membrane disruption and polymer aggregation, greatly reducing the DPPC main

Table 2 Calorimetric profiles of DPPC:PNIPAM-b-PLA 1 chimeric bilayers in PBS (pH = 7.4) (2nd heating cycle)

Sample	Molar ratio	$T_{onset,m}$/°C	T_m/°C	$\Delta T_{1/2,m}$/°C	ΔH_m/J g^{-1}	$T_{onset,s}$/°C	T_s/°C	$\Delta T_{1/2,s}$/°C	ΔH_s/J g^{-1}	$T_{onset,t}$/°C	T_t/°C	$\Delta T_{1/2,t}$/°C	ΔH_t/J g^{-1}
Lipid	–	41.05	41.88	1.45	−44.88	34.60	36.54	2.06	−4.78	–	–	–	–
Chimeric	9:0.02	40.78	41.43	1.17	−50.22	34.09	36.12	2.06	−5.41	–	–	–	–
Chimeric	9:0.05	40.74	41.40	1.13	−48.43	33.62	35.69	2.32	−4.50	–	–	–	–
Chimeric	9:0.1	40.69	41.49	1.26	−39.55	33.22	35.22	2.39	−2.19	26.28	27.90	2.05	−1.82
Chimeric	9:0.2	40.66	41.45	1.22	−30.62	33.34	35.24	2.26	−1.31	26.02	27.82	2.21	−3.84
Chimeric	9:0.5	40.46	41.26	1.35	−16.86	–	–	–	–	25.82	27.81	2.34	−6.93
Chimeric	9:1	40.27	41.17	1.38	−8.25	44.79	46.36	1.72	−2.57	25.51	27.61	2.49	−10.42
Polymer	–	–	–	–	–	–	–	–	–	25.63	27.97	2.78	−7.03

T_{onset}: temperature at which the thermal event starts; T: temperature at which heat capacity (ΔC_p) at constant pressure is maximum; $\Delta T_{1/2}$: width at half peak height of the transition; ΔH: transition enthalpy normalized per gram of chimeric system. m: main transition; s: secondary transition; t: thermoresponsive transition

transition, creating a new phase above the main transition and increasing the thermoresponsive transition. This is the only studied chimeric system with all these phases present on a single curve. The 1st cooling scan was consistent with the 2nd heating scan, indicating that after the 1st heating, the new phases were in equilibrium and all non-reversible phenomena had ended (Figure S2 and Table S1). This is also evident from the cooling thermodynamic parameters, which were close to those of the 2nd heating. During the cooling process, the main transition temperature presented a slight hysteresis, the main transition enthalpy was slightly higher, and the thermoresponsive transition of PNIPAM appeared in higher temperature and also appeared for 9:0.05. The unique phase of 9:1 was observed, however could not be integrated, because it was very close to the main transition, practically as a shoulder.

Concerning PNIPAM-b-PLA 2, with molecular weight 6400 and relative block composition 50–50%, this copolymer is more hydrophobic in terms of its relative composition and hydrophilic-to-hydrophobic balance; however, it is lower in total mass. These two parameters might have an unpredictable effect on the thermotropic behavior of DPPC membranes, compared with PNIPAM-b-PLA 1 (Fig. 3 and Tables 3, 4). At first glance, all thermotropic effects seem less intense than before. Polymer molar ratios up to 9:0.2 produce a slight thermotropic effect on DPPC membranes, leading to chimeric system 9:1, where a new phase has been clearly developed. However, this happened from polymer ratios as low as 9:0.2 in the case of PNIPAM-b-PLA 1 and additionally, we did not observe any shoulders on the main transition for this case, except maybe for 9:0.5. These shoulders are indicators of inhomogeneous distribution of phases inside the phospholipid membrane, with probable clusters of polymer in various sites, what tends to lead to the phenomenon of "phase separation" [39]. What we can say for both polymers is that there is no clear phase separation near the main transition for any polymer amount during the 1st heating cycle (Figs. 2a, 3a). Only during the 2nd cycle and for chimeric systems DPPC:PNIPAM-b-PLA 1 or 2 9:1 (Figs. 2b, 3b), we can distinguish the creation of two high temperature phases on the same curve. Regarding the main transition enthalpy, it was in all chimeric system cases lower than the reference lipid system and this reduction was less acute than the first polymer, confirming that the polymer architecture defines the intensity of the thermotropic effect (Figure S1B). The same applies on the 2nd heating cycle and additionally, the thermoresponsive enthalpy reduction from 1st to 2nd is almost nonexistent, indicating that the PNIPAM segment, which is much longer in the case of PNIPAM-b-PLA 1, due to both polymer composition and molecular weight, is responsible for the membrane-disruptive behavior and creation of a new, low-temperature transition. Correlation analysis gave for both heating cycles

Table 3 Calorimetric profiles of DPPC:PNIPAM-b-PLA 2 chimeric bilayers in PBS (pH = 7.4) (1st heating cycle)

Sample	Molar ratio	$T_{onset,m}$/°C	T_m/°C	$\Delta T_{1/2,m}$/°C	ΔH_m/J g^{-1}	$T_{onset,s}$/°C	T_s/°C	$\Delta T_{1/2,s}$/°C	ΔH_s/J g^{-1}
Lipid	–	41.04	41.80	−44.60	−44.60	35.16	36.62	1.86	−5.81
Chimeric	9:0.02	41.25	42.21	−52.88	−42.93	33.37	35.83	2.69	−3.08
Chimeric	9:0.05	41.05	41.95	−51.05	−34.02	33.87	35.73	2.16	−1.75
Chimeric	9:0.1	41.15	42.15	−44.72	−46.93	32.65	35.11	2.67	−2.16
Chimeric	9:0.2	40.93	41.93	−39.28	−45.87	–	–	–	–
Chimeric	9:0.5	40.79	42.57	−25.55	−38.64	–	–	–	–
Chimeric	9:1	42.30	44.85	−17.00	−27.89	–	–	–	–
Polymer	–	–	–	–	–	–	–	–	–

T_{onset}: temperature at which the thermal event starts; T: temperature at which heat capacity (ΔC_p) at constant pressure is maximum; $\Delta T_{1/2}$: width at half peak height of the transition; ΔH: transition enthalpy normalized per gram of chimeric system. m: main transition; s: secondary transition

Table 4 Calorimetric profiles of DPPC:PNIPAM-b-PLA 2 chimeric bilayers in PBS (pH = 7.4) (2nd heating cycle)

Sample	Molar ratio	$T_{onset,m}$/°C	T_m/°C	$\Delta T_{1/2,m}$/°C	ΔH_m/J g^{-1}	$T_{onset,s}$/°C	T_s/°C	$\Delta T_{1/2,s}$/°C	ΔH_s/J g^{-1}
Lipid	–	41.05	41.88	−44.88	−44.88	34.60	36.54	2.06	−4.78
Chimeric	9:0.02	41.03	41.86	−50.22	−41.72	33.77	35.49	2.21	−2.67
Chimeric	9:0.05	40.84	41.51	−48.43	−33.52	33.68	35.23	1.90	−1.93
Chimeric	9:0.1	40.85	41.62	−39.55	−45.47	33.21	34.95	2.03	−2.17
Chimeric	9:0.2	40.65	41.39	−30.62	−44.25	32.77	34.39	1.91	−1.07
Chimeric	9:0.5	40.45	41.39	−16.86	−36.56	–	–	–	–
Chimeric	9:1	40.46	41.51	−8.25	−25.83	–	–	–	–
Polymer	–	–	–	–	–	–	–	–	–

T_{onset}: temperature at which the thermal event starts; T: temperature at which heat capacity (ΔC_p) at constant pressure is maximum; $\Delta T_{1/2}$: width at half peak height of the transition; ΔH: transition enthalpy normalized per gram of chimeric system. m: main transition; s: secondary transition

a linear dependence, which is an interesting feature for such dynamic nanosystems and has been observed previously for other systems as well (Fig. 4b) [19].

Regarding the pretransition in the case of PNIPAM-b-PLA 2, it is present up to molar ratio 9:0.1 for the 1st heating and also reappears for 9:0.2 during the 2nd. Another interesting finding is the shoulder that is visible above the main transition in the case of cooling for systems 9:0.2, 0.5 and 1 (Figure S3 and Table S2). This was only verified during 2nd heating for 9:1 and contrary with PNIPAM-b-PLA 1, where it was visible for 9:1, it could mean that the polymer-grafted membrane responds during cooling as well, affecting the polymer conformation inside and in these cases requires both heating and cooling to adopt its final organization. This phase is possibly hidden inside the main transition during the 1st heating of both polymers, was distinguished during cooling, especially for PNIPAM-b-PLA 2 and finally led to phase separation for the molar ratio 9:1. In lower polymer concentrations, the thermoresponsive main transition led to a single phase at these temperatures. To summarize, the effect of PNIPAM is much different in the case of PNIPAM-b-PLA 2, because of no thermoresponsive reduction of the main transition enthalpy, as well as lack of a transition close to the LCST of PNIPAM and these phenomena are expected if we take into account the lack of transition for the neat polymer sample. Consequently, the thermodynamic effect of the polymer on DPPC membranes is also polymer composition dependent, apart from concentration dependent. The length of individual segments, PNIPAM and PLA, and overall molecular weight are key factors for the insertion, conformation inside the membrane and final functionality, which determine the biophysical behavior of these chimeric membranes [40].

Our first conclusion is that these chimeric nanosystems are indeed thermoresponsive and they require heating above their main phase transition in order to reach an equilibrium state, producing an effect that could be called "phase functionality." This behavior might be the main parameter to modulate their biophysical behavior in vivo. However, their initial non-equilibrium and metastable phase is what makes them unique as aDDnSs and potential nanocarriers of drug molecules, or other therapeutics [20]. This is because for the first time, it is evident that the functionality of nanosystems and especially stimuli-responsive ones hides inside temporary thermodynamic states, which in this case are temperature-dependent. Functionality is set off by the membrane

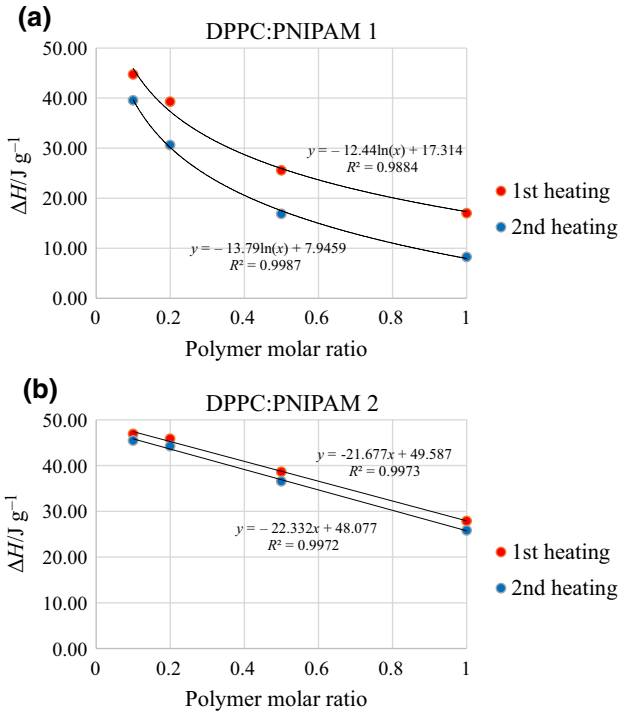

Fig. 4 Regression analysis plots of transition specific enthalpy (ΔH_m) versus the concentration of the incorporated polymer for **a** DPPC:PNIPAM-b-PLA 1 **b** DPPC:PNIPAM-b-PLA 2

phase transition, which allows for polymer lateral diffusion, phase segregation and formation of hydrophobic polymer domains inside the bilayer. At the same time, it is defined by the polymer phase transition, which less hydrophilic at high temperatures and tends to aggregate [13, 35]. These states are tools of bio-functionality, and their analysis on a thermodynamic basis is the first step toward the delineation of the biophysics of stimuli-responsive chimeric nanosystems [28].

Physicochemical Characteristics and Colloidal Stability of Chimeric Liposomes

Chimeric/mixed liposomes comprised of DPPC, EPC and the two thermoresponsive amphiphilic diblock copolymers were developed in certain lipid/polymer molar ratios, and their physicochemical properties are presented in Table 5. In addition, the physical colloidal stability of the liposomes, in terms of size and polydispersity, is presented in Figure S4 and S5, respectively.

Initially, thermoresponsive chimeric liposomes composed of DPPC and PNIPAM-b-PLA 1 or 2 were constructed. The size and polydispersity for DPPC were around 50 nm and 0.2, respectively. The zeta potential was estimated close to zero. Concerning the chimeric nanosystems, those were developed by incorporating increasing concentration of each copolymer inside the liposomal membrane. This

Table 5 Physicochemical characteristics of DPPC/EPC conventional and DPPC/EPC:PNIPAM-b-PLA 1/2 chimeric systems in PBS

Sample	Molar ratio	D_h^1/nm	SD[2]	PDI[3]	SD	z-pot[4]/mV	SD
DPPC	–	53.8	0.9	0.235	0.010	2.3	1.1
DPPC:PNIPAM-b-PLA 1	9:0.02	114.0	4.0	0.549	0.058	0.1	0.5
DPPC:PNIPAM-b-PLA 1	9:0.05	113.7	3.1	0.574	0.009	−0.2	0.7
DPPC:PNIPAM-b-PLA 1	9:0.1	103.2	2.5	0.596	0.008	0.9	0.5
DPPC:PNIPAM-b-PLA 1	9:0.5	286.3	4.3	1.000	0.000	–	–
DPPC:PNIPAM-b-PLA 2	9:0.02	337.8	7.4	1.000	0.000	–	–
DPPC:PNIPAM-b-PLA 2	9:0.05	355.8	33.5	1.000	0.000	–	–
DPPC:PNIPAM-b-PLA 2	9:0.1	131.7	2.6	0.381	0.012	−6.4	0.3
DPPC:PNIPAM-b-PLA 2	9:0.5	286.3	4.3	1.000	0.000	–	–
EPC	–	92.0	2.9	0.440	0.006	−2.4	1.5
EPC:PNIPAM-b-PLA 1	9:0.02	97.1	1.2	0.365	0.020	−5.6	2.1
EPC:PNIPAM-b-PLA 1	9:0.1	127.9	0.6	0.280	0.022	−1.0	1.4
EPC:PNIPAM-b-PLA 1	9:0.5	Aggr[5]	Aggr	Aggr	Aggr	Aggr	Aggr
EPC:PNIPAM-b-PLA 2	9:0.02	89.1	0.4	0.437	0.006	−5.0	0.5
EPC:PNIPAM-b-PLA 2	9:0.1	74.3	1.2	0.257	0.036	−11.8	1.6
EPC:PNIPAM-b-PLA 2	9:0.5	80.6	4.4	0.320	0.055	−13.2	2.5

[1]Hydrodynamic diameter
[2]Standard deviation
[3]Polydispersity index
[4]Zeta potential
[5]Aggregates

integration led to physicochemical properties that were polymer composition dependent, but not polymer concentration dependent, contrary to previous investigations [19, 21]. In particular, the copolymer of higher molecular weight and of more hydrophilic composition, i.e., percentage in PNIPAM segments, allowed for formulation of lipid/polymer nanosystems of various molar ratios, while the one of lower weight and more hydrophobic balance could only be successfully incorporated at one specific molar ratio. Namely, for DPPC:PNIPAM-b-PLA 1 chimeric systems, molar ratios of 9:0.02, 9:0.05 and 9:0.1 led to self-assembly of the biomaterials to nanostructures of size between 100–115 nm and polydispersity 0.5–0.6, while for DPPC:PNIPAM-b-PLA 2, only 9:0.1 lipid-to-polymer ratio led to structures of promising physicochemical properties, that is size around 130 nm and polydispersity of 0.4 (Table 5). This difference between the two cases highlights the fact that not only the length of the hydrophobic anchor of a copolymer, but also the whole polymer size and relative balance between hydrophilic and hydrophobic segments are very crucial parameters for chimeric liposomal system development. The rest of the chimeric systems, DPPC:PNIPAM-b-PLA 1 9:0.5, DPPC:PNIPAM-b-PLA 2 9:0.02, 9:0.05 and 9:0.5, self-assembled into totally heterogeneous populations of large aggregates. As a result, we did not attempt to prepare liposomes with higher amount of polymers, due to their hydrophobic character rendering the hydration process impossible and producing aggregates. The zeta potential of all chimeric systems that had no aggregates and thus could be measured was close to zero, with only DPPC:PNIPAM-b-PLA 2 9:0.1 exhibiting slightly negative charge, presumably attributed to the carboxyl group –COOH of the copolymers being ionized at this pH (7.4).

EPC was also utilized for chimeric liposomal formulations. Neat EPC liposomes had a size of 90 nm and polydispersity near 0.4. The zeta potential was also close to zero in this case as well. Regarding the EPC-containing chimeric nanosystems, we utilized three different concentrations of each thermoresponsive copolymer. As expected, the different mass and composition of the two copolymers defined the self-assembly process and led to different results in each case. Interestingly, in the case of EPC, PNIPAM-b-PLA 2 exhibited higher cooperativity with the phospholipid. This is evident from the smaller size of EPC:PNIPAM-b-PLA 2 nanoparticles (75–90 nm), compared with EPC:PNIPAM-b-PLA 1 (95–130 nm), as well as from the fact that EPC could incorporate successfully the highest amount of PNIPAM-b-PLA 2 (9:0.5), while PNIPAM-b-PLA 1 led to aggregates. The zeta potential of most chimeric liposomes was slightly negative, owed to the ionized carboxyl group $–COO^-$ of the copolymers and EPC:PNIPAM-b-PLA 2 exhibited a polymer-concentration-dependent charged surface, going from − 5 mV to up to − 13 mV.

Finally, the physical colloidal stability of the chimeric nanosystems was tested and is presented in Figure S4 for size and Figure S5 for polydispersity. Concerning DPPC, conventional liposomes underwent a size increase that tripled their diameter from 60 nm to 180 nm, due to aggregation phenomena and membrane fusion, while chimeric systems more or less preserved their properties (Figure S4A and S5A). On the other hand, EPC liposomes did not increase as much in size as DPPC ones, apparently due to their initial size being larger, with lower surface free energy and lower tendency to aggregate. The chimeric liposomes with EPC were physically stable only in the case of PNIPAM-b-PLA 1 (Figure S4B and S5B). Judging from both DPPC and EPC cases, the stabilizing role of PNIPAM-b-PLA 1 (66–34%, 18,000) definitely exists in the chimeric liposomal systems. Even though their zeta potential was around zero for all nanosystems and electrostatic interactions were minimum, the incorporated polymers formed a corona around the membranes, which in certain cases provided colloidal stability through steric repulsion. Specifically, the hydrophobic PLA segment is incorporated inside the bilayers, while the hydrophilic PNIPAM chains extend around the liposomal membrane and promote the entropic effect, osmotic effect and enthalpic stabilization each time two nanoparticles approach one another, maintaining the stability of the system [41, 42]. It is most probable that in the case of PNIPAM-b-PLA 2 (50–50%), this mechanism does not prevail, because of the less hydrophilic character of the copolymer, as well as its overall lower molecular mass (6400), which means that the hydrophilic chains are much shorter than in the case of PNIPAM-b-PLA 1.

Cryo-TEM Imaging of Chimeric Liposomes

Chimeric liposomal formulations consisting of DPPC or EPC and PNIPAM-b-PLA 1 were analyzed with cryo-TEM, in order to assess the self-assembled nanoparticle nature and morphology. Previous investigations have discussed how the individual biomaterials' properties, as well as their relative molar ratio and total concentration may affect the final structure formation and the equilibrium state of membranes inside the colloidal dispersion [21, 43]. Herein, cryo-TEM images of DPPC:PNIPAM-b-PLA 1 9:0.05, EPC:PNIPAM-b-PLA 1 9:0.02 and EPC:PNIPAM-b-PLA 1 9:0.1 are provided in Fig. 5.

Concerning DPPC:PNIPAM-b-PLA 1 9:0.05, the pictures in Fig. 5a reveal the nature, size and morphology of nanostructures. In particular, we observed the existence of vesicles, with membrane thickness around 5–6 nm and size 10–100 nm and below. Some unclosed membranes were also present, as well as a few multiwall/multilamellar particles with diameter 200–350 nm. The effects of faceting and contrast-heterogeneity are seen on the membrane of liposomes

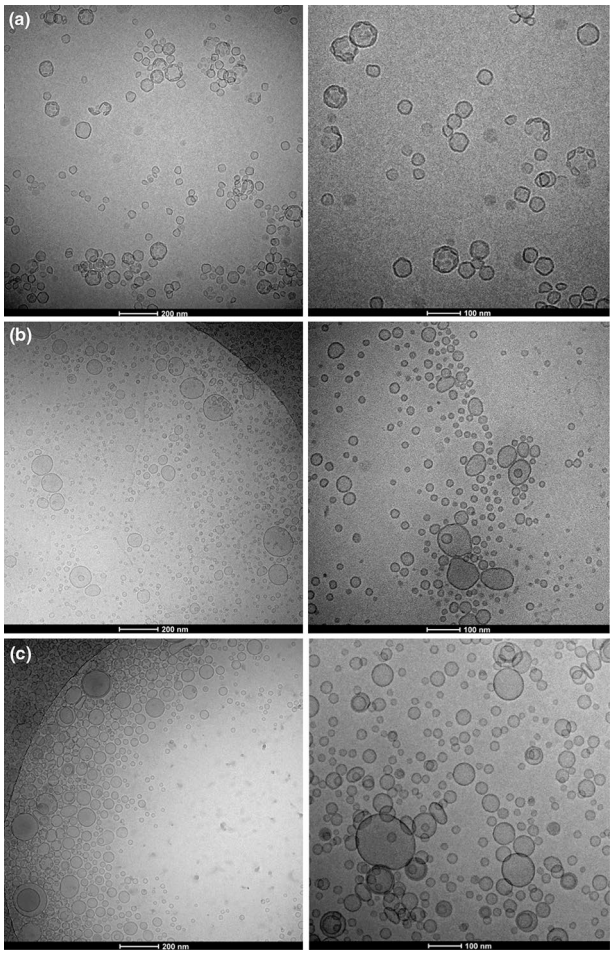

Fig. 5 Cryo-TEM images of aggregates of **a** DPPC:PNIPAM-PLA 1 9:0.05, **b** EPC:PNIPAM-PLA 1 9:0.02 and **c** EPC:PNIPAM-PLA 1 9:0.1 chimeric systems

as "irregularities" and according to the literature, they are common phenomena in chimeric nanosystems, attributed to either the technique conditions or to the existence of anchored polymer molecules onto the membranes, which promote the formation of nanodomains [43–47]. The most interesting finding in this case of chimeric nanosystem was the co-existence of normal-looking membranes and membranes that exhibited a "football-like" surface, like vesicles growing from another vesicle. This behavior is expected, due to the different hydrophilic-to-hydrophobic balance of the phospholipid and the copolymer or as documented, the mismatch between the molecules. This "incompatibility" leads to mismatch between the thickness of lipid and polymer membranes, finally promoting the formation of domains of one biomaterial inside the other, characterized by a hydrophobic mismatch on the boundaries, which energetically stabilizes the domains. Another scenario is that these domains are of lipidic nature and are stabilized by the copolymer at the boundaries [46, 48, 49]. However, these mechanisms have been associated with large vesicular structures, i.e., a few micrometers, and not liposomes of 100 nm size. We assume that the smaller the size, the most difficult it is for such areas to form upon membranes, due to high curvature and energetic disfavor. On top of that, we did not find an image of similar-looking nanoparticles, especially referring to the high curvature of domains existing on the membranes, forming a morphology that is rather unique.

The chimeric nanosystems incorporating EPC and PNIPAM-b-PLA 1, in molar ratios 9:0.02 and 9:0.1, are presented in Fig. 5b, c, respectively. Both these systems presented only vesicles of membrane thickness 3–4 nm. Particles have been classified to two categories of hydrodynamic diameter, 10–150 nm and larger particles of hydrodynamic diameter that exceeds 200 nm. Contrary with DPPC, these nanosystems were homogeneous in terms of membrane morphology and no football-like structures were observed. As a result, we conclude that the different phospholipid and the lyotropism between the biomaterials, i.e., the self-assembly behavior based on the individual molecule properties and concentration, are the parameters that promote the morphogenesis of these structures [50]. In these cases, we also observed no membrane irregularities, what may be associated with the low phase transition temperature of EPC and probably indicating the homogeneous distribution of polymer inside the liposomal membrane [51].

Summarizing, all the studied chimeric nanosystems were homogeneous in terms of membrane morphology and self-assembled into vesicles and not into other morphologies, such as "worm-like" or "disk-like" micelles, which have been previously observed for similar systems [43]. These vesicles are characterized by membrane thickness between 3 and 6 nm, being close to the documented 3–5 nm for conventional liposomes and membranes [52]. Consequently, they are mainly liposomes and not polymersomes, whose membrane thickness is between 10 and 50 nm, based on the hydrophobic segment and molecular weight of the polymer [53]. Polymer insertion inside the liposomal membrane may induce an increase in the membrane thickness, which explains why some vesicle membranes reached 6 nm [54]. Nevertheless, since no other morphologies are present and the self-assembled membranes are indicative of liposomal formation, we conclude that the amphiphilic copolymers are attached on the membranes, either homogeneously distributed or in nanodomains, depending on the utilized phospholipid and the biomaterial concentration.

Thermoresponsiveness of Chimeric Liposomes

In order to assess the concentration-dependent thermoresponsive effect of the polymers on the membranes, we utilized the chimeric liposomes composed of DPPC and

PNIPAM-b-PLA 1. The formulations of molar ratios 9:0.02, 0.05 and 0.1 were tested for alteration of their physicochemical properties during day 10 post-preparation, after heating for 30 min at 45 °C (above the main transition temperature observed for the 1st heating scan through DSC), as well as after probe sonication. The stages before heating, after heating, after reaching room temperature and after heating again are depicted in Fig. 6a, alongside a proposed mechanism on the nanosystems' behavior (Fig. 6b). The results regarding the hydrodynamic diameter and polydispersity are presented in Fig. 7, while the corresponding intensity plots are provided in Figure S6.

First of all, DPPC liposomes were exposed to increased temperature conditions for 30 min, where bilayers existed in the liquid crystalline phase (L_α) and as a result, were more fluid and susceptible to membrane fusion during vesicular contact. This led to a slight hydrodynamic diameter (D_h) and polydispersity (PDI) increase, from 180 nm to 200 nm and from 0.35 to 0.42, respectively. The particular behavior was expected, and after probe sonication, the vesicles returned to their initial physicochemical properties [55].

Compared with conventional liposomes, the response of the chimeric nanosystems to heating was more profound. The suspensions of chimeric liposomes went from homogeneous and uniformly blur to biphasic, containing in each case one, large hydrophobic agglomerate/aggregate, surrounded by transparent suspension (Fig. 6a). This phenomenon is indicative of phase separation inside the systems, attributed to the tendency of PNIPAM chains to expel molecules of water from their surrounding environment and promote the switch of hydrophilic surfaces to hydrophobic when exposed to temperature that exceeds the phase transition temperature [35]. These surfaces in turn approach one another, because they thermodynamically avoid contact with the aqueous phase and the membrane stabilizing mechanisms are reversed (Fig. 6b) [11, 41]. As a result, a single and large agglomerate/aggregate is created, which is partially reversible, if left to anneal and reach room temperature again [56]. Afterward, we observed that by heating again, the heat-driven effect that was produced was not exactly the same. In particular, DPPC:PNIPAM-b-PLA 9:0.02 led to almost the same result as before; however, the two higher in polymer amount systems did not, especially the one with the highest. Instead, they looked almost unaffected after heated a second time. This means that at low polymer concentration, the new phase and liposomal structure are mostly reversible after the 1st heating, because the number of polymer molecules onto the membrane is not enough to permanently alter them, and therefore, the same result is produced after a 2nd heating. As the polymer increases, the impact of thermoresponsive behavior of PNIPAM affects significantly the liposomal

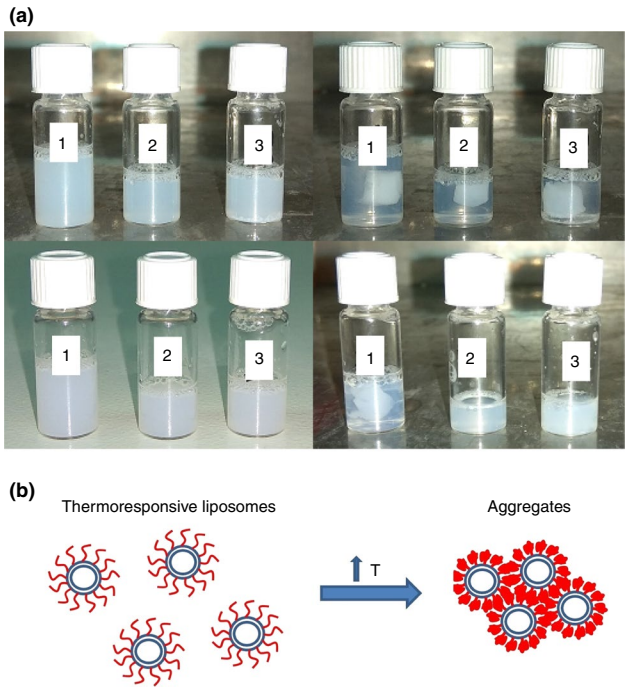

Fig. 6 **a** DPPC:PNIPAM-b-PLA 1 chimeric liposomes during day 10 at room temperature (upper left), after heating (upper right), after reaching room temperature (down left) and after heating again (down right) and **b** illustration of the thermoresponsive aggregation of chimeric liposomes. Sample 1: DPPC:PNIPAM-b-PLA 9:0.02; Sample 2: DPPC:PNIPAM-b-PLA 9:0.05; Sample 3: DPPC:PNIPAM-b-PLA 9:0.1

membrane, leading to permanent disruption after the 1st heating process [6, 33]. This is a polymer-concentration-dependent effect that is also confirmed by the DSC results discussed earlier.

Specifically, the particle size of chimeric nanosystems was profoundly affected after heating the formulations at 45 °C and leaving them to anneal at room temperature (Fig. 7a). For DPPC:PNIPAM-b-PLA 1 9:0.02, it increased from 130 nm to around 400 nm, for 9:0.05 it went up to 520 nm, and finally, for 9:0.1 it reached almost 1000 nm. In all cases, the homogeneity of the system was minimum after heating, with PDI values being always maximum (Fig. 7b). These measurement results verify the polymer-concentration-dependent liposomal aggregation and membrane disruption that occur after stimulating the thermoresponsive systems [6, 31]. As more polymer molecules are incorporated inside the membrane, the agglomeration and aggregation phenomena increase and greatly affect the physicochemical properties of liposomes, especially in the case of molar ratio 9:0.1. In contrast, the reference DPPC liposomes did not exhibit such hydrodynamic diameter and polydispersity differences after exposure to increased temperature. Therefore, the functionality of the incorporated

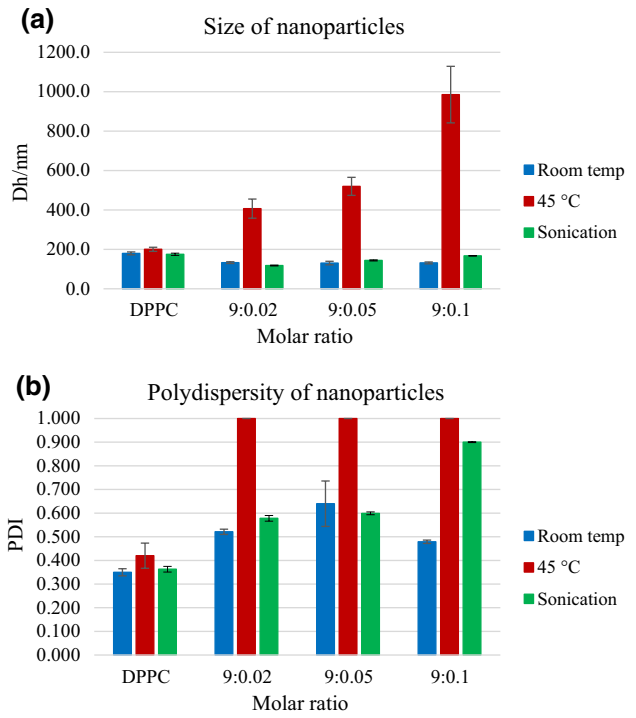

Fig. 7 Physicochemical characteristics, regarding **a** size and **b** polydispersity, of DPPC:PNIPAM-b-PLA 1 chimeric systems during day 10 in room temperature, after heating at 45 °C and after probe sonication

thermoresponsive copolymer on the liposomal membranes exists and is manifested through alteration of the hydrophilic surface around liposomes and consequent agglomeration via hydrophobic interactions between these surfaces [35]. Finally, the chimeric nanosystems were subjected again to sonication, in order to re-disperse them in the aqueous medium. The results of this attempt were in agreement with DSC, since higher polymer concentration inside liposomal membranes led to permanent disruption after the 1st heating process, which could not be reversed by sonication. In particular, we were able to revert the aggregation effect on DPPC:PNIPAM-b-PLA 1 9:0.02 and 9:0.05, but not so much for 9:0.1, which ultimately had size around 170 nm and polydispersity close to maximum 0.9.

The metastable phase that is created by inserting thermoresponsive copolymer chains inside the membrane is of similar energetic content with DPPC membranes in the case of DPPC:PNIPAM-b-PLA 9:0.02, not so similar for 9:0.05 and different for 9:0.1 [20]. From DSC results, it was evident that this phase becomes more present as more copolymer is incorporated inside the bilayer and melts at higher temperature. It was also evident that if transition occurs, the available energetic content leads to a non-reversible process and a distinct thermoresponsive behavior, which is observed for liposomes as well. That content is defined by the information-to-entropy balance between the two utilized biomaterial, inside specific lyotropic conditions of concentration and relative molar concentration. These in turn lead to self-assembly and morphogenesis of liposomal structures, where the copolymer resides inside the membranes in a certain conformation that is stable but may induce dynamic effects if stimulated properly [43, 50].

Conclusions

Chimeric/mixed bilayers and liposomes consisting of DPPC or EPC and PNIPAM-b-PLA copolymers of different molecular characteristics were designed, developed and studied through various methods. The DSC results suggest the organization and creation of a new functional phase inside the membrane, which follows a polymer-concentration- and composition-dependent manner. From the physicochemical results, it is evident that the copolymer PNIPAM-b-PLA 1 stabilizes better the liposomal membrane in certain amounts and no more than 9:0.1. This restriction is correlated with the lyotropic effect that this component has on membranes, meaning that its chemistry and concentration in the chimeric system define its final conformation inside the liposomal membrane. Cryo-TEM revealed the morphological characteristics of the nanoparticles, indicating homogeneous vesicular systems, with the interesting finding of "football-like" membranes for DPPC:PNIPAM-b-PLA 1 9:0.05. Finally, the thermoresponsive behavior of chimeric liposomes after heating was in agreement with DSC results and suggested an agglomeration and aggregation effect, which occurs once and alters permanently the membrane properties, with impact on the particle size and polydispersity.

The critical parameter and driving force for the creation and behavior of functional phases is the lyotropism of the utilized biomaterials, which depends on their molecular properties, such as hydrophilic-to-hydrophobic balance, as well as on their concentration inside the chimeric system. The composition- and concentration-dependent lyotropic effect of thermoresponsive copolymers on phospholipid membranes defines the self-assembly process and depending on the system's information-to-entropy balance, leads to morphogenesis of specific structures with certain physicochemical properties and functional behavior. These nanostructures possess chimeric and innovative properties, such as "phase functionality," that originate from the combined properties of membranes and polymers, however, are completely new. Overall, polymer incorporation produces functional non-equilibrium/metastable and non-reversible structures and phases with specific information/energy content and information-to-entropy balance, and by heating, we can induce their functionality, which in turn shifts

this balance to an equilibrium state. The interpretation of the thermoresponsiveness and functionality in general of chimeric/mixed nanosystems on the basis of biophysics and thermodynamics is mandatory to fully realize how these systems work and will impact greatly the field of drug delivery, offering utilities that will lead to improved clinical effectiveness and safety.

Acknowledgements The research work was supported by the Hellenic Foundation for Research and Innovation (HFRI) and the General Secretariat for Research and Technology (GSRT), under the HFRI PhD Fellowship grant (GA. no. 392). We would also like to thank Dimitrios Fessas, Associate Professor in the Department of Food, Environmental and Nutritional Sciences—DeFENS, University of Milan, for his valuable advice on interpreting the DSC results and thermodynamic behavior of thermoresponsive chimeric nanosystems. In Poland, this work was supported by state funds for the Centre of Polymer and Carbon Materials, Polish Academy of Science.

Compliance with ethical standards

Conflict of interest The authors declare that they have no conflict of interest.

References

1. Demetzos C, Pippa N. Advanced drug delivery nanosystems (aDDnSs): a mini-review. Drug Deliv. 2014;21:250–7.
2. Naziris N, Pippa N, Pispas S, Demetzos C. Stimuli-responsive drug delivery nanosystems: from bench to clinic. Curr Nanomed. 2016;6:1–20.
3. Dou Y, Hynynen K, Allen C. To heat or not to heat: challenges with clinical translation of thermosensitive liposomes. J Control Release. 2017;249:63–73.
4. Kneidl B, Peller M, Winter G, Lindner LH, Hossann M. Thermosensitive liposomal drug delivery systems: state of the art review. Int J Nanomed. 2014;9:4387–98.
5. Lee Y, Thompson DH. Stimuli-responsive liposomes for drug delivery. Wiley Interdiscip Rev Nanomed Nanobiotechnol. 2017. https://doi.org/10.1002/wnan.1450.
6. Lee SM, Nguyen ST. Smart nanoscale drug delivery platforms from stimuli-responsive polymers and liposomes. Macromolecules. 2013;46:9169–80.
7. Sánchez-Moreno P, de Vicente J, Nardecchia S, Marchal JA, Boulaiz H. Thermo-sensitive nanomaterials: recent advance in synthesis and biomedical applications. Nanomaterials (Basel). 2018;8:935–66.
8. Hongshua B, Jianxiu X, Hong J, Shan G, Dongjuan T, Yan F, Kai S. Current developments in drug delivery with thermosensitive liposomes. Asian J Pharm. 2019;14:365–79.
9. Heskins M, Guillet JE. Solution properties of poly(*n*-isopropylacrylamide). J Macromol Sci. 1968;2:1441–55.
10. Futscher MH, Philipp M, Müller-Buschbaum P, Schulte A. The role of backbone hydration of poly(*n*-isopropyl acrylamide) across the volume phase transition compared to its monomer. Sci Rep. 2017;7:17012–31.
11. Pelton R. Poly(N-isopropylacrylamide) (PNIPAM) is never hydrophobic. J Colloid Interface Sci. 2010;348:673–4.
12. Southall NT, Dill KA, Haymet ADJ. A view of the hydrophobic effect. J Phys Chem B. 2002;106:521–33.
13. Liu P, Song L, Li N, Lin J, Huang D. Time dependence of phase separation enthalpy recovery behavior in aqueous poly(*N*-isopropylacrylamide) solution. J Therm Anal Calorim. 2017;130:843–50.
14. Lanzalaco S, Armelin E. Poly(*n*-isopropylacrylamide) and copolymers: a review on recent progresses in biomedical applications. Gels. 2017;3:36–67.
15. Ward MA, Georgiou TK. Thermoresponsive polymers for biomedical applications. Polymers. 2011;3:1215–42.
16. Liu R, Fraylich M, Saunders BR. Thermoresponsive copolymers: from fundamental studies to applications. Colloid Polym Sci. 2009;287:627–43.
17. Eeckman F, Moës AJ, Amighi K. Synthesis and characterization of thermosensitive copolymers for oral controlled drug delivery. Eur Polym J. 2004;40:873–81.
18. Demetzos C. Differential scanning calorimetry (DSC): a tool to study the thermal behavior of lipid bilayers and liposomal stability. J Liposome Res. 2008;18:159–73.
19. Naziris N, Pippa N, Stellas D, Chrysostomou V, Pispas S, Demetzos C, Libera M, Trzebicka B. Development and evaluation of stimuli-responsive chimeric nanostructures. AAPS PharmSciTech. 2018;19:2971–89.
20. Naziris N, Demetzos C. The role of the information/entropy balance in self-assembly. The structural hierarchy of chimeric drug delivery nanosystems. Pharmakeftiki. 2017;19:77–82.
21. Pippa N, Pispas S, Demetzos C. The metastable phases as modulators of biophysical behavior of liposomal membranes. J Therm Anal Calorim. 2015;120:937–45.
22. Pippa N, Stellas D, Skandalis A, Pispas S, Demetzos C, Libera M, Marcinkowski A, Trzebicka B. Chimeric lipid/block copolymer nanovesicles: physico-chemical and bio-compatibility evaluation. Eur J Pharm Biopharm. 2016;107:295–309.
23. Ionov M, Klajnert B, Gardikis K, Hatziantoniou S, Palecz B, Salakhutdinov B, Cladera J, Zamaraeva M, Demetzos C, Bryszewska M. Effect of amyloid beta peptides $A\beta_{1-28}$ and $A\beta_{25-40}$ on model lipid membranes. J Therm Anal Calorim. 2010;99:741–7.
24. Gardikis K, Hatziantoniou S, Signorelli M, Pusceddu M, Micha-Screttas M, Schiraldi A, Demetzos C, Fessas D. Thermodynamic and structural characterization of Liposomal-Locked in-Dendrimers as drug carriers. Colloids Surf B Biointerfaces. 2010;81:11–9.
25. Kolman I, Pippa N, Meristoudi A, Pispas S, Demetzos C. A dual-stimuli-responsive polymer into phospholipid membranes. J Therm Anal Calorim. 2016;123:2257–71.
26. Pippa N, Chronopoulos DD, Stellas D, Fernández-Pacheco R, Arenal R, Demetzos C, Tagmatarchis N. Design and development of multi-walled carbon nanotube-liposome drug delivery platforms. Int J Pharm. 2017;528:429–39.
27. Pippa N, Meristoudi A, Pispas S, Demetzos C. Temperature-dependent drug release from DPPC:C12H25-PNIPAM-COOH liposomes: control of the drug loading/release by modulation of the nanocarriers' components. Int J Pharm. 2015;485:374–82.
28. Demetzos C. Biophysics and thermodynamics: the scientific building blocks of bio-inspired drug delivery nano systems. AAPS PharmSciTech. 2015;16:491–5.
29. Ali S, Minchey S, Janoff A, Mayhew E. A differential scanning calorimetry study of phosphocholines mixed with paclitaxel and its bromoacylated taxanes. Biophys J. 2000;78:246–56.
30. Bruggemann EP, Melchior DL. Alterations in the organization of phosphatidylcholine/cholesterol bilayers by tetrahydrocannabinol. J Biol Chem. 1983;258:8298–303.
31. Fujisawa S, Kadoma Y, Ishihara M, Atsumi T, Yokoe I. Dipalmitoylphosphatidylcholine (DPPC) and DPPC/cholesterol liposomes as predictors of the cytotoxicity of bis-GMA related compounds. J Liposome Res. 2004;14:39–49.
32. Koynova R, Caffrey M. Phases and phase transitions of the phosphatidylcholines. Biochim Biophys Acta. 1998;1376:91–145.

33. Sadozai H, Saeidi D. Recent developments in liposome-based veterinary therapeutics. ISRN Vet Sci. 2013;2013.
34. Pippa N, Gardikis K, Pispas S, Demetzos C. The physicochemical/thermodynamic balance of advanced drug liposomal delivery systems. J Therm Anal Calorim. 2014;116:99–105.
35. Kono K. Thermosensitive polymer-modified liposomes. Adv Drug Deliv Rev. 2001;53:307–19.
36. Spěváček J, Konefał R, Dybal J, Čadová E, Kovářová J. Thermoresponsive behavior of block copolymers of PEO and PNIPAm with different architecture in aqueous solutions: a study by NMR, FTIR, DSC and quantum-chemical calculations. Eur Pol J. 2017;94:471–83.
37. Zhang Y, Furyk S, Sagle LB, Cho Y, Bergbreiter DE, Cremer PS. Effects of Hofmeister anions on the LCST of PNIPAM as a function of molecular weight. J Phys Chem C Nanomater Interfaces. 2007;111:8916–24.
38. Binder WH, Barragan V, Menger FM. Domains and rafts in lipid membranes. Angew Chem Int Ed Engl. 2003;42:5802–27.
39. Matsingou C, Demetzos C. Calorimetric study on the induction of interdigitated phase in hydrated DPPC bilayers by bioactive labdanes and correlation to their liposome stability: the role of chemical structure. Chem Phys Lipids. 2007;145:45–62.
40. Itel F, Chami M, Najer A, Lörcher S, Wu D, Dinu IA, Meier W. Molecular organization and dynamics in polymersome membranes: a lateral diffusion study. Macromolecules. 2014;47:7588–96.
41. Attwood D, Florence AT. Physical pharmacy. 2nd ed. London: Pharmaceutical Press; 2012.
42. Kono K, Nakai R, Morimoto K, Takagishi T. Thermosensitive polymer-modified liposomes that release contents around physiological temperature. Biochim Biophys Acta. 1999;1416:239–50.
43. Naziris N, Pippa N, Chrysostomou V, Pispas S, Demetzos C, Libera M, et al. Morphological diversity of block copolymer/lipid chimeric nanostructures. J Nanopart Res. 2017;19:347–57.
44. Kaiser N, Kimpfler A, Massing U, Burger AM, Fiebig HH, Brandl M, Schubert R. 5-Fluorouracil in vesicular phospholipid gels for anticancer treatment: entrapment and release properties. Int J Pharm. 2003;256:123–31.
45. Bowick MJ, Sknepnek R. Pathways to faceting of vesicles. Soft Matter. 2013;9:8088–95.
46. Dao TPT, Fernandes F, Er-Rafik M, Salva R, Schmutz M, Brûlet A, Prieto M, Sandre O, Le Meins JF. Phase separation and nanodomain formation in hybrid polymer/lipid vesicles. ACS Macro Lett. 2015;4:182–6.
47. Fox CB, Mulligan SK, Sung J, Dowling QM, Fung HW, Vedvick TS, Coler RN. Cryogenic transmission electron microscopy of recombinant tuberculosis vaccine antigen with anionic liposomes reveals formation of flattened liposomes. Int J Nanomed. 2014;9:1367–77.
48. Le Meins JF, Schatz C, Lecommandoux S, Sandre O. Hybrid polymer/lipid vesicles: state of the art and future perspectives. Mater Today. 2013;16:397–402.
49. Chemin M, Brun PM, Lecommandoux S, Sandre O, Le Meins JF. Hybrid polymer/lipid vesicles: fine control of the lipid and polymer distribution in the binary membrane. Soft Matter. 2012;8:2867–74.
50. Lim SK, Wong ASW, de Hoog HPM, Rangamani P, Parikh AN, Nallani M, Sandin S, Liedberg B. Spontaneous formation of nanometer scale tubular vesicles in aqueous mixtures of lipid and block copolymer amphiphiles. Soft Matter. 2017;13:1107–15.
51. Rangelov S, Edwards K, Almgren M, Karlsson G. Steric stabilization of egg-phosphatidylcholine liposomes by copolymers bearing short blocks of lipid-mimetic units. Langmuir. 2003;19:172–81.
52. Kuntsche J, Horst JC, Bunjes H. Cryogenic transmission electron microscopy (cryo-TEM) for studying the morphology of colloidal drug delivery systems. Int J Pharm. 2011;417:120–37.
53. Le Meins JF, Sandre O, Lecommandoux S. Recent trends in the tuning of polymersomes' membrane properties. Eur Phys J E Soft Matter. 2011;34:14–31.
54. Schulz M, Binder WH. Mixed hybrid lipid/polymer vesicles as a novel membrane platform. Macromol Rapid Commun. 2015;36:2031–41.
55. Roy B, Guha P, Bhattarai R, Nahak P, Karmakar G, Chettri P, Panda AK. Influence of lipid composition, pH, and temperature on physicochemical properties of liposomes with curcumin as model drug. J Oleo Sci. 2016;65:399–411.
56. Nichols G, Byard S, Bloxham MJ, Botterill J, Dawson NJ, Dennis A, Diart V, North NC, Sherwood JD. A review of the terms agglomerate and aggregate with a recommendation for nomenclature used in powder and particle characterization. J Pharm Sci. 2002;91:2103–9.